

# A Zoo of Strange Attractors from the Canonical Chua's Circuits

L.O.Chua

University of California Berkeley

## Abstract

By adding a linear resistor  $R_0$  in Chua's circuit, we obtain an immensely richer bifurcation landscape, including an endowment of more than 20 new distinct strange attractors which were suppressed when  $R_0 \rightarrow 0$ . We interpret this augmented circuit as a *global unfolding* of Chua's circuit because its basic mechanism is similar to the local unfolding theory in nonlinear mathematics.

Moreover, this augmented Chua's circuit, which has only 7 parameters, is canonical in the sense that it is capable of duplicating all qualitative behaviors of a 21-parameter family  $\mathcal{C}$  of ordinary differential equations in  $R^3$ .

Explicit formulas are given for calculating the 7 circuit parameters of the augmented Chua's circuit so that it is topologically conjugate (i.e., equivalent) to any member of this 21-parameter family of 3rd-order piecewise-linear circuits; namely, the Chua's circuit family. This paper closes with a gallery of selected strange attractors from this canonical circuit.

## 1 Introduction

Let  $\mathcal{C}$  denote the family of all continuous, odd-symmetric, 3-region piecewise-linear vector fields in  $R^3$ . By changing coordinates if necessary, there is no loss of generality to assume that the affine regions are bounded by two planes:  $x = 1$  and  $x = -1$ , respectively. Such vector fields can be described by

$$\begin{aligned} \begin{bmatrix} \dot{x} \\ \dot{y} \\ \dot{z} \end{bmatrix} &= \underbrace{\begin{bmatrix} a_{11} & a_{12} & a_{13} \\ a_{21} & a_{22} & a_{23} \\ a_{31} & a_{32} & a_{33} \end{bmatrix}}_{\mathbf{A}_0} \begin{bmatrix} x \\ y \\ z \end{bmatrix}, \text{ if } |x| \leq 1 \\ &= \underbrace{\begin{bmatrix} \hat{a}_{11} & \hat{a}_{12} & \hat{a}_{13} \\ \hat{a}_{21} & \hat{a}_{22} & \hat{a}_{23} \\ \hat{a}_{31} & \hat{a}_{32} & \hat{a}_{33} \end{bmatrix}}_{\mathbf{A}_1} \begin{bmatrix} x \\ y \\ z \end{bmatrix} + \begin{bmatrix} b_1 \\ b_2 \\ b_3 \end{bmatrix}, \text{ if } |x| > 1 \end{aligned} \quad (1)$$

Observe that Eq.(1) is characterized by 21 parameters ( $a_{ij}, \hat{a}_{ij}, b_i, i, j = 1, 2, 3$ ). This family corresponds to the class of vector fields studied in [1-2], and includes the equations describing Chua's circuit [3], and the canonical circuit realization in [4], as special cases. The circuit given in [4] is *canonical* in the sense that given any vector field belonging to  $\mathcal{C}$ , there exists a

set of circuit parameters such that the corresponding circuit in [4] exhibits the same qualitative behaviors, and no circuit having fewer circuit elements has this property. The proof of this property is based on the fundamental normal form theorem proved in [1] which asserts that two vector fields in  $\mathcal{C}$  are *equivalent*, i.e., topologically conjugate, if and only if corresponding matrices  $\mathbf{A}_0$  and  $\mathbf{A}_1$  have *identical eigenvalues*.

There exist many other circuits which can be shown also to be canonical [5]. In this paper, we will single out the canonical circuit shown in Fig. 1 because it is obtained by adding a linear resistor in series with the inductor L in Chua's circuit. Here, the nonlinear resistor is described by an odd-symmetric 3-segment  $v_R - i_R$  characteristic (Fig.1(b)) described by

$$i_R = f(v_R) = G_b v_R + \frac{1}{2}(G_a - G_b)[|v_R + B_p| - |v_R - B_p|] \quad (2)$$

where  $G_a$  and  $G_b$  are the slopes of the inner and outer segments, respectively.

The break point voltage  $B_p$  can be normalized to unity, without changing the circuit's qualitative behaviors. Mathematically, we can interpret the augmented circuit in Fig.1 as a global unfolding of Chua's circuit. In this sense, we can state that the two canonical circuits in [4] and Fig.1 are global unfoldings of the only two viable chaotic circuit candidates derived in [3].

Although other canonical circuits in [5] may be preferred for *specific* applications, as dictated by the practicability of the corresponding circuit parameters, from the pedagogical and historical point of view, we will henceforth focus our attention to this new canonical circuit. Our main goal in this paper is to unify all previously investigated members of Chua's circuit family [6-13] and produce the circuit parameters for this new canonical circuit in order to obtain the corresponding bifurcation behaviors and/or chaotic attractors.

In *Section 2* we will present the explicit formulas for calculating the circuit parameters for this new canonical circuit, as well as for its dimensionless form.

In *Section 3*, we will apply the formulas from *Section 2* to reproduce the qualitative behaviors of all previously published results on Chua's circuit family. We will then select a subset of the most interesting strange attractors from this tedious but worthwhile exercise and present them in the form of a gallery of strange attractors.

## 2 State Equations and Explicit Formulas for Equivalent Circuit Parameters

The state equation for the canonical Chua's circuit in Fig.1 is given by:

$$\begin{aligned} \frac{dv_1}{dt} &= \frac{1}{C_1} \left[ \frac{v_2 - v_1}{R} - f(v_1) \right] \\ \frac{dv_2}{dt} &= \frac{1}{C_2} \left[ \frac{v_1 - v_2}{R} + i_3 \right] \\ \frac{di_3}{dt} &= \frac{1}{L} [-v_2 - R_0 i_3] \end{aligned} \quad (3)$$

where  $f(v_1)$  is given by Eq.(2). Since we can assume  $B_p = 1$  without changing the qualitative behavior, the dynamics of this circuit is uniquely characterized by only 7 parameters; namely,  $C_1, C_2, L, R_1, R_0, G_a,$  and  $G_b$ .

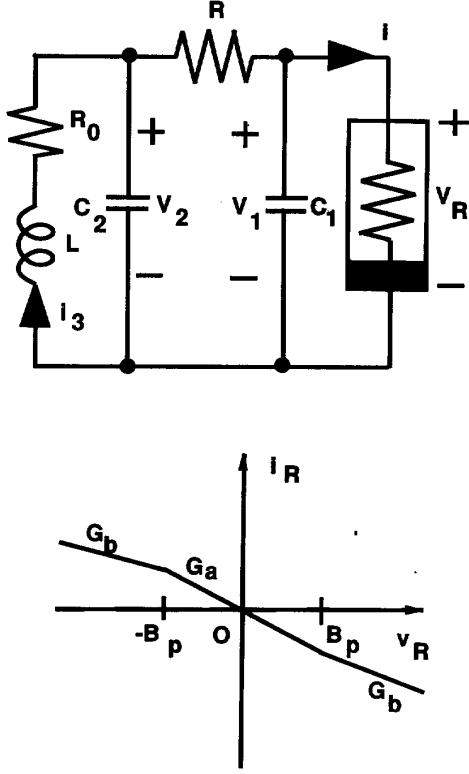


**Fig.1 Canonical circuit obtained by a global unfolding of Chua's circuit and the nonlinear characteristic.**

By following exactly the same reasoning and procedures given in [4], we can prove that this circuit is canonical. In particular, let  $\{\mu_1, \mu_2, \mu_3\}$  denote the eigenvalues of  $\mathbf{A}_0$  in the inner region  $D_0$ , defined by  $|x| \leq 1$ , and let  $\{\nu_1, \nu_2, \nu_3\}$  denote the eigenvalues of  $\mathbf{A}_1$  in the odd-symmetric outer regions  $D_{+1}$  and  $D_{-1}$ . These eigenvalues can be arbitrarily specified except that complex eigenvalues are assumed to occur in complex-conjugate pairs. Consequently, we can transform these (possibly complex) eigenvalues into the following equivalent set of 6 real numbers:

$$\begin{aligned} p_1 &= \mu_1 + \mu_2 + \mu_3 \\ p_2 &= \mu_1\mu_2 + \mu_2\mu_3 + \mu_3\mu_1 \\ p_3 &= \mu_1\mu_2\mu_3 \end{aligned} \quad (4)$$

$$\begin{aligned} q_1 &= \nu_1 + \nu_2 + \nu_3 \\ q_2 &= \nu_1\nu_2 + \nu_2\nu_3 + \nu_3\nu_1 \\ q_3 &= \nu_1\nu_2\nu_3 \end{aligned} \quad (5)$$

Since it is more convenient to work with real numbers, we will, without loss of generality, refer to  $\{p_1, p_2, p_3, q_1, q_2, q_3\}$  as our eigenvalue specifications. Since two identical linear circuits with different impedance scalings have identical eigenvalues, we need at least 7 circuit parameters in order to calculate them uniquely to match a given set of eigenvalue parameters. The circuit in Fig.1 has the minimum number of parameters needed. We fix the impedance level by assuming for convenience  $C_1 = 1$ .

From this, we can prove the canonical property of the circuit in Fig.1 by a constructive method; namely by deriving the formulas for the remaining 6 parameters explicitly, as in [4]. We now collect these formulas as follow:

$$C_1 = 1 \quad (6)$$

$$R = \frac{-p_2 + q_2}{p_1 - q_1} k + (p_1 + \frac{-p_2 + q_2}{p_1 - q_1}) \frac{p_3 - q_3}{p_1 - q_1} k^2 - p_3 k^2 \quad (7)$$

$$C_2 = \frac{k}{R^2} \quad (8)$$

$$L = \frac{C_2}{\frac{1}{R^2} + C_2^2 \frac{p_3 - q_3}{p_1 - q_1} - \frac{-p_2 + q_2}{p_1 - q_1} \frac{C_2}{R}} \quad (9)$$

$$R_0 = R \left( \frac{p_3 - q_3}{p_1 - q_1} C_2 L - 1 \right) \quad (10)$$

$$G_a = -p_1 - \frac{-p_2 + q_2}{p_1 - q_1} - \frac{1}{R} \quad (11)$$

$$G_b = -q_1 - \frac{-p_2 + q_2}{p_1 - q_1} - \frac{1}{R} \quad (12)$$

where

$$k \triangleq \frac{1}{-p_2 - \left( \frac{p_2 - q_2}{p_1 - q_1} - p_1 \right) \frac{p_2 - q_2}{p_1 - q_1} + \frac{p_3 - q_3}{p_1 - q_1}}$$

Observe that there is a set of eigenvalues of measure zero (e.g., when any denominator in Eqs.(6)-(12) is zero) for which Eqs.(6)-(12) are undefined. In such cases, we can invoke the fundamental theorem of differential equations which asserts that the solution is a continuous function of its parameters. Consequently, we can make arbitrarily small perturbations of such eigenvalues without changing the qualitative behavior of the original circuit. It is these perturbed eigenvalues parameters that we use in calculating the circuit parameters in Fig.1. This perturbation does not affect our claim of canonical property because our circuit in Fig. 1 is only required to have the same qualitative behaviors, not the same eigenvalues as the member of the 21-parameter Chua's circuit family.

Since usually we are only interested in the qualitative behaviors of the canonical circuit, we can rescale time to eliminate one of the parameters in Eq.(3), as well as rescaling the variables to obtain the following equivalent dimensionless system:

$$\begin{aligned} \frac{dx}{d\tau} &= \alpha[y - x - f(x)] \\ \frac{dy}{d\tau} &= x - y + z \\ \frac{dz}{d\tau} &= -\beta y - \gamma z \end{aligned} \quad (13)$$

where

$$f(x) = bx + \frac{1}{2}(a - b)[|x + 1| - |x - 1|]$$

or equivalently

$$f(x) = \begin{cases} bx + a - b & \text{if } x \geq 1 \\ ax & \text{if } |x| \leq 1 \\ bx - a + b & \text{if } x \leq -1 \end{cases} \quad (14)$$

The dimensionless variables and parameters are defined as follows:

$$x \triangleq v_1/B_p \quad y \triangleq v_2/B_p \quad z \triangleq i_3 \left( \frac{R}{B_p} \right) \quad (15)$$

$$\alpha \triangleq C_2/C_1 \quad \beta \triangleq \frac{R^2 C_2}{L} \quad \gamma \triangleq \frac{R R_0 C_2}{L} \quad (16)$$

$$a \triangleq R G_a \quad b \triangleq R G_b \quad (17)$$

And the dimensionless time is

$$\tau \triangleq \frac{t}{RC_2} \quad (18)$$

Observe that the dimensionless time  $\tau$  is negative if either  $R < 0$  or  $C_2 < 0$ . In either case, the dynamics of the dimensionless equation (13) are identical to those of the Eq.(13) by integrating Eq.(13) *backwards* in time. If we prefer to integrate in the usual times, as when calling a standard integration subroutine, we need only introduce one more parameter  $\sigma$  and use the following equivalent system:

$$\begin{aligned} \dot{x} &= \sigma\alpha[y - x - f(x)] \\ \dot{y} &= \sigma[x - y + z] \\ \dot{z} &= \sigma[-\beta y - \gamma z] \end{aligned}$$

where

$$\sigma = \begin{cases} 1 & \text{if } RC_2 > 0 \\ -1 & \text{if } RC_2 < 0 \end{cases}$$

Here the dot  $\dot{\phantom{x}}$  denotes differentiation with respect to the dimensionless time  $\tau$ .

### 3 Translating Previous Bifurcation Parameters and Phenomena into the New Canonical Chua's Circuit

#### 3.1 Intermittency Route to Chaos

Figs. 2-7 show a series of Lissajou's figures obtained from the circuit. When we start from  $L = -0.00744$ , the  $v_1 - v_2$  figure is a symmetric limit cycle (Fig.2). As  $L$  decreases and reaches a critical value, this symmetric limit cycle splits into two asymmetric limit cycles, which are symmetric to each other. As  $L$  decreases further, *intermittency* eventually occurs (Fig.3). The waveform associated with the trajectory consists of a long regular phase and is followed by a short burst. As  $L$  decreases further, the regular phases get shorter and the bursts appear more frequently (Fig.4). The waveform looks completely chaotic. As  $L$  decreases further, half of the attractor suddenly disappears as shown in Fig.5. This chaotic attractor will gradually shrink and eventually become a periodic limit cycle (Fig.7). Fig.6 shows a period-2 limit cycle.

#### 3.2 Torus Breakdown

We start from  $C_1 = 5$ , when the corresponding  $v_1 - v_2$  figure is a limit cycle (Fig.8). As  $C_1$  decreases and reaches a critical value the periodic attractor has undergone a Hopf bifurcation, thereby giving birth to a two-torus(Fig.9). As we decrease  $C_1$  further we observed that the two-torus and periodic attractor (phase-locking) alternatively appear and disappear many times. Fig.10 gives a sample of some of the periodic attractors. As  $C_1$  further decreases we found a folded torus (Fig.11). It is rather interesting to observe that a further decrease of  $C_1$  resulted in the two folded tori merging together and giving rise to a double scroll attractor (Fig.13). In Fig.12 we show a periodic window.

## 4 A Gallery of Strange Attractors

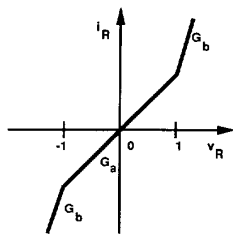
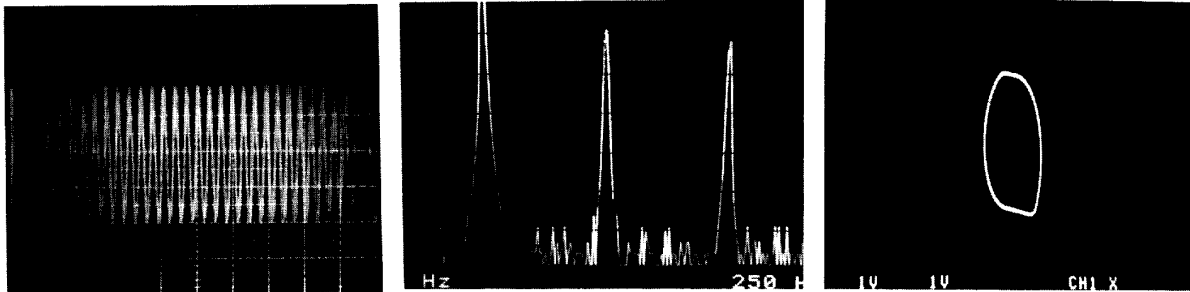
In Figs.15-25 we present a gallery of strange attractors.

#### Acknowledgement

I would like to thank Profs. Lj.Kocarev and A.S. Huang for deriving the explicit formulas and for calculating the equivalent circuit parameters, as well as for collecting the strange attractors in Section 4. This work is supported in part by the National Science Foundation under Grant MIP 89-12639, and by the Office of Naval Research under Grant N00014-89-J-1402.

#### References

- [1] L.O.Chua, M.Komuro, and T.Matsumoto, "The double scroll family, parts I and II," *IEEE Trans CAS*, vol. 33, no. 11, pp. 1073-1118, 1986.
- [2] S.Wu, "Chua's circuit family," *Proc. of the IEEE*, vol. 75, no. 8, pp. 1022-1032, 1987.
- [3] L.O.Chua, "The genesis of Chua's circuit," *Archiv fur Elektronik und Ubertragungstechnik*, vol. 46, no. 4, pp. 250-257, 1992.
- [4] L.O.Chua and G.N.Lin, "Canonical realization of Chua's circuit family," *IEEE Trans CAS*, vol. 37, no. 7, pp. 885-902, 1990.
- [5] L.Kocarev, A.S.Huang, Lj.Karadzinov, and L.O.Chua, "A catalog of all canonical piecewise-linear circuits belonging to Chua's circuit family," Tech. Rep. M92/80, Electronic Research Laboratory, UCB/ERL, September 15,1992.
- [6] L.O.Chua, M.Komuro, T.Matsumoto, L.O.Chua, and R.Tokunaga, "Chaos via torus breakdown," *IEEE Trans CAS*, vol. 34, no. 3, pp. 240-253, 1987.
- [7] T.S.Parker and L.O.Chua, "The double scroll equation," *IEEE Trans CAS*, vol. 34, no. 9, pp. 1059-1073, 1988.
- [8] C.P.Silva and L.O.Chua, "The overdamped double scroll family," *Int.J.Circuit Theory Appl.*, vol. 16, no. 3, pp. 223-302, 1988.
- [9] P.Bartissol and L.O.Chua, "The double hook," *IEEE Trans CAS*, vol. 35, no. 12, pp. 1512-1522, 1988.
- [10] L.O.Chua and G.N.Lin, "Intermittency in a piecewise-linear circuit," *IEEE Trans CAS*, vol. 38, no. 5, pp. 510-520, 1990.
- [11] G.N.Lin and L.O.Chua, "Nonfractal chaotic attractor in a 2-dimensional surface," Tech. Rep. M91/32, Electronic Research Laboratory University of California Berkeley, March 1,1991.
- [12] R.W.Brockett, "On conditions leading to chaos in feedback systems," in *Proc. CDS*, December 1982.
- [13] M.J.Ogorzalek, "Order and chaos in a third-order RC ladder network with nonlinear feedback," *IEEE Trans CAS*, vol. 36, no. 9, pp. 1221-1230, 1989.



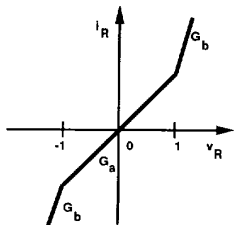
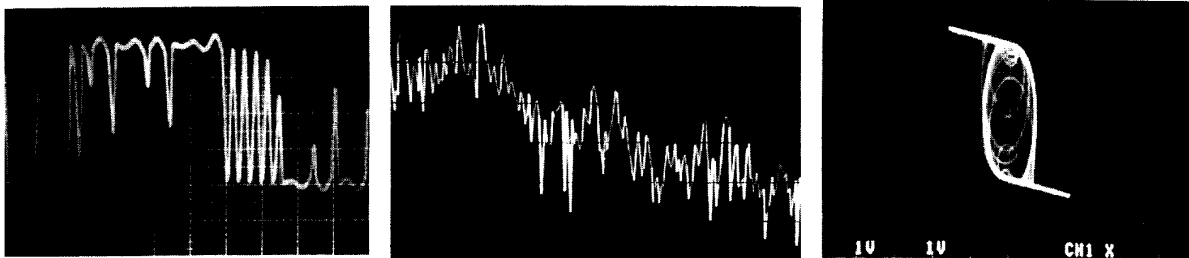
PARAMETERS:  $C_1=1$ ,  $C_2=-75$ ,  $G_a=14.7$ ,  $G_b=36$

$R=.066667$ ,  $R_0=.006667$ ,  $L=-.00744$

LYAPUNOV EXPONENTS:  $\lambda_1=0$ ,  $\lambda_2=-.01$ ,  $\lambda_3=-5.39$

**Fig.2** Time waveform, spectrum of the signal, phase-plot observed for the indicated nonlinear characteristic and the set of parameters.

Corresponding Lyapunov exponents are also given.

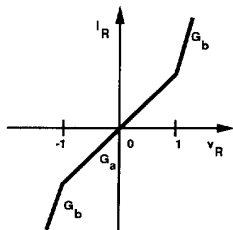
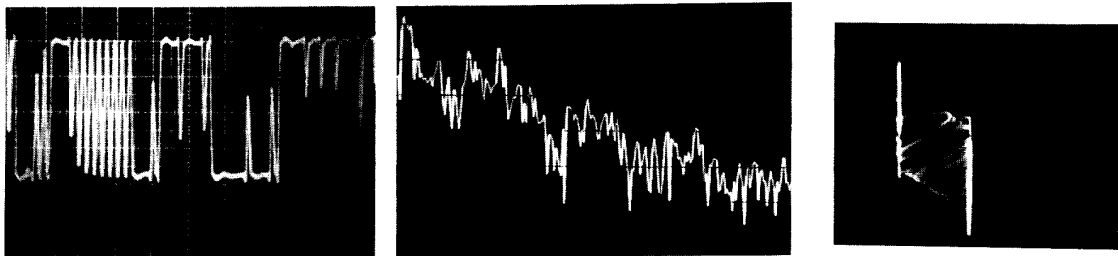


PARAMETERS:  $C_1=1$ ,  $C_2=-75$ ,  $G_a=14.7$ ,  $G_b=36$

$R=.066667$ ,  $R_0=.006667$ ,  $L=-.0096$

LYAPUNOV EXPONENTS:  $\lambda_1=.25$ ,  $\lambda_2=0$ ,  $\lambda_3=-12.40$

**Fig.3** Experimental results (see the caption of Fig.2 for explanation) for the set of parameters as indicated.

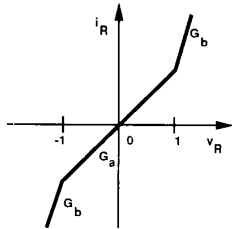
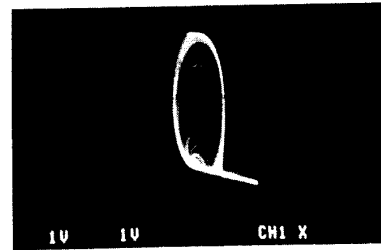
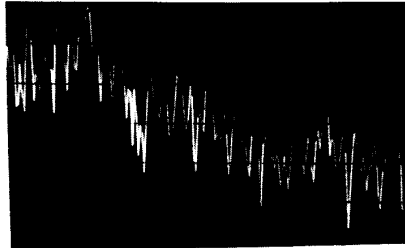
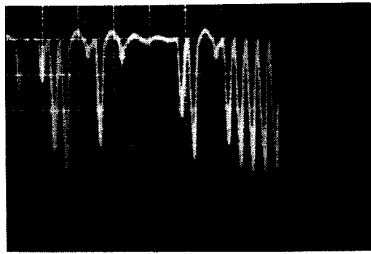


PARAMETERS:  $C_1=1$ ,  $C_2=-75$ ,  $G_a=14.7$ ,  $G_b=36$

$R=.066667$ ,  $R_0=.006667$ ,  $L=-.0105$

LYAPUNOV EXPONENTS:  $\lambda_1=.18$ ,  $\lambda_2=0$ ,  $\lambda_3=-11.70$

**Fig.4** Experimental results (see the caption of Fig.2 for explanation) for the set of parameters as indicated.

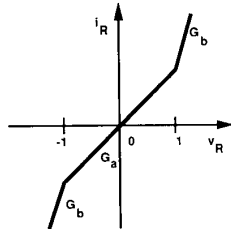
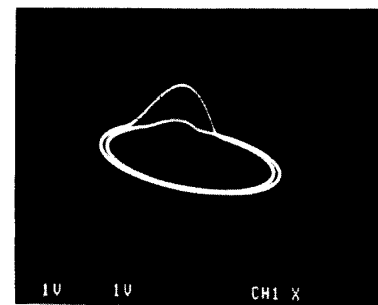
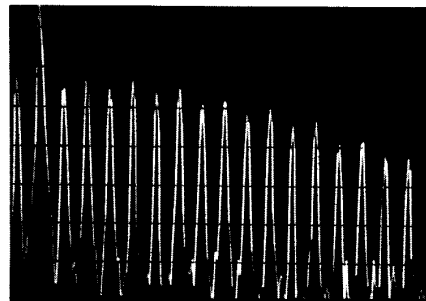
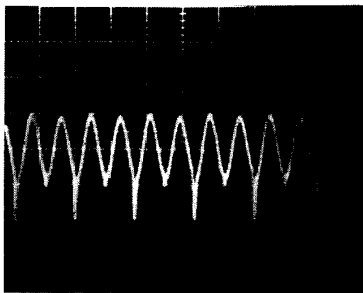


PARAMETERS:  $C_1=1$ ,  $C_2=-75$ ,  $G_a=14.7$ ,  $G_b=36$

$R=.066667$ ,  $R_0=.006667$ ,  $L=-.010666$

LYAPUNOV EXPONENTS:  $\lambda_1=.21$ ,  $\lambda_2=0$ ,  $\lambda_3=-14.16$

**Fig.5** Experimental results (see the caption of Fig.2 for explanation) for the set of parameters as indicated.

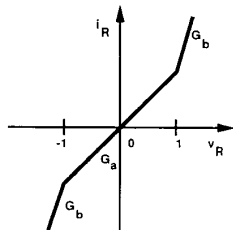
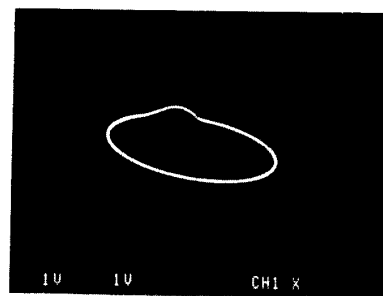
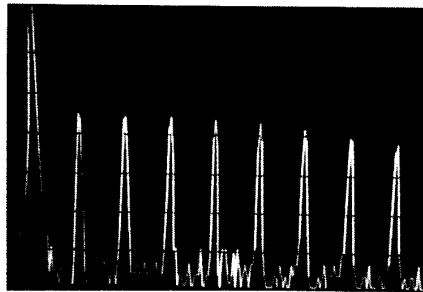
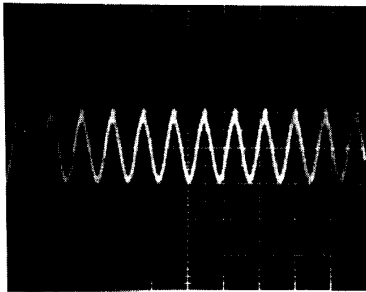


PARAMETERS:  $C_1=1$ ,  $C_2=-75$ ,  $G_a=14.7$ ,  $G_b=36$

$R=.066667$ ,  $R_0=.006667$ ,  $L=-.0018133$

LYAPUNOV EXPONENTS:  $\lambda_1=0$ ,  $\lambda_2=-.06$ ,  $\lambda_3=-17.30$

**Fig.6** Experimental results (see the caption of Fig.2 for explanation) for the set of parameters as indicated.

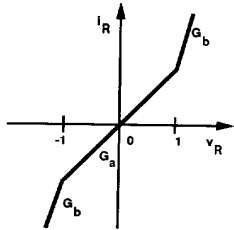
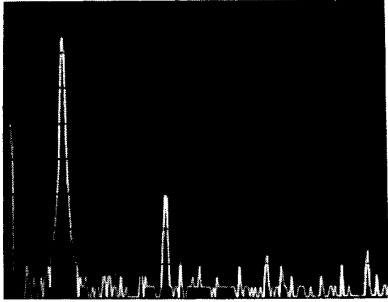
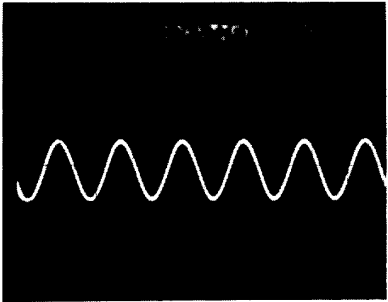


PARAMETERS:  $C_1=1$ ,  $C_2=-75$ ,  $G_a=14.7$ ,  $G_b=36$

$R=.066667$ ,  $R_0=.006667$ ,  $L=-.019$

LYAPUNOV EXPONENTS:  $\lambda_1=0$ ,  $\lambda_2=-.16$ ,  $\lambda_3=-17.94$

**Fig.7** Experimental results (see the caption of Fig.2 for explanation) for the set of parameters as indicated.

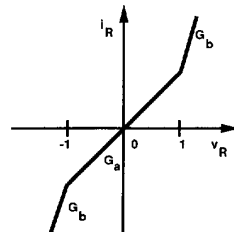
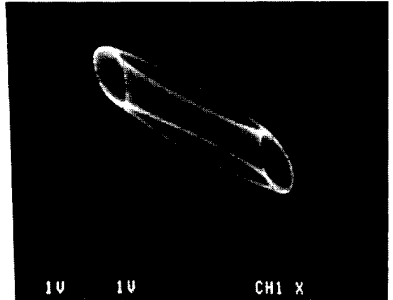
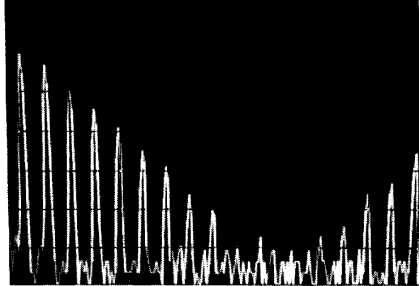
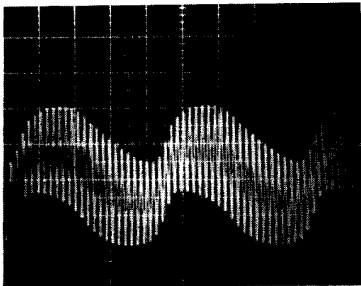


PARAMETERS:  $C_1=5$ ,  $C_2=100$ ,  $G_a=.599$ ,  $G_b=.77$

$R=.000929$ ,  $R_0=-1.4286$ ,  $L=.136$

LYAPUNOV EXPONENTS:  $\lambda_1=0$ ,  $\lambda_2=-.01$ ,  $\lambda_3=-.02$

**Fig.8** Experimental results (see the caption of Fig.2 for explanation) for the set of parameters as indicated.

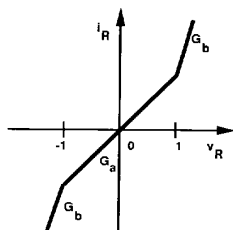
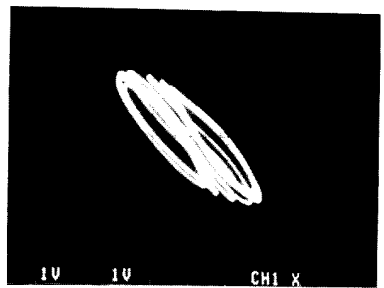
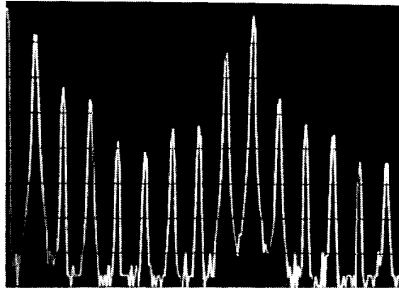
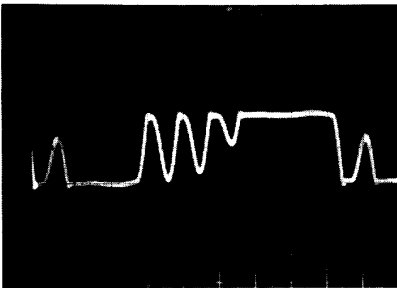


PARAMETERS:  $C_1=1$ ,  $C_2=100$ ,  $G_a=.599$ ,  $G_b=.77$

$R=.000929$ ,  $R_0=-1.4286$ ,  $L=.136$

LYAPUNOV EXPONENTS:  $\lambda_1=0$ ,  $\lambda_2=0$ ,  $\lambda_3=-.01$

**Fig.9** Experimental results (see the caption of Fig.2 for explanation) for the set of parameters as indicated.

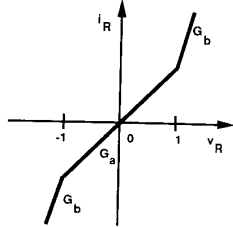
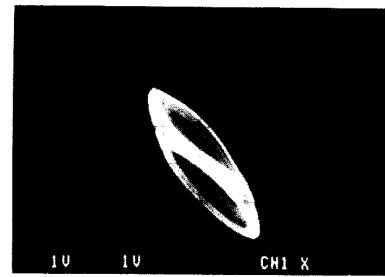
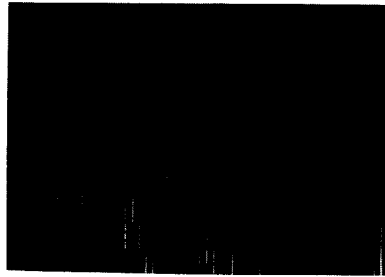
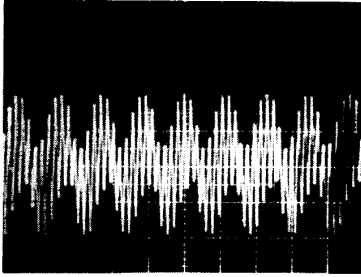


PARAMETERS:  $C_1=.6$ ,  $C_2=100$ ,  $G_a=.599$ ,  $G_b=.77$

$R=.000929$ ,  $R_0=-1.4286$ ,  $L=.136$

LYAPUNOV EXPONENTS:  $\lambda_1=0$ ,  $\lambda_2=-.01$ ,  $\lambda_3=-.02$

**Fig.10** Experimental results (see the caption of Fig.2 for explanation) for the set of parameters as indicated.

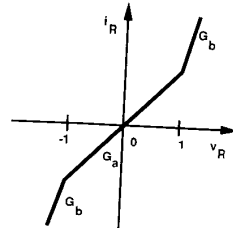
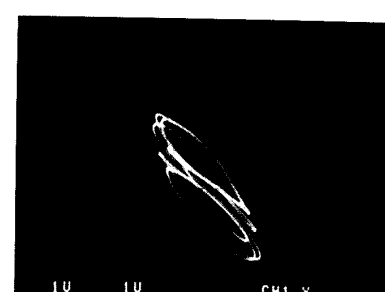
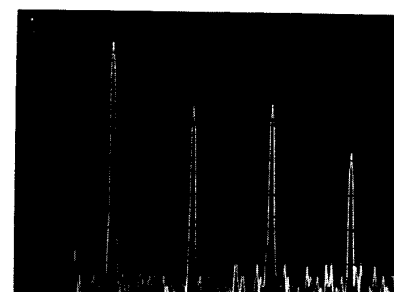
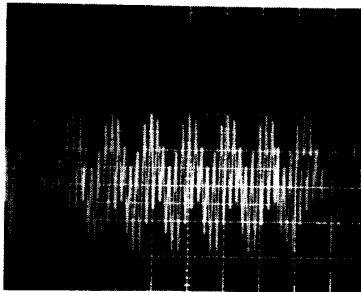


PARAMETERS:  $C_1 = .51$ ,  $C_2 = 100$ ,  $G_a = .599$ ,  $G_b = .77$

$R = .000929$ ,  $R_0 = -1.4286$ ,  $L = .136$

LYAPUNOV EXPONENTS:  $\lambda_1 = .01$ ,  $\lambda_2 = 0$ ,  $\lambda_3 = -.02$

Fig.11 Experimental results (see the caption of Fig.2 for explanation) for the set of parameters as indicated.

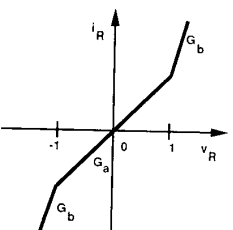
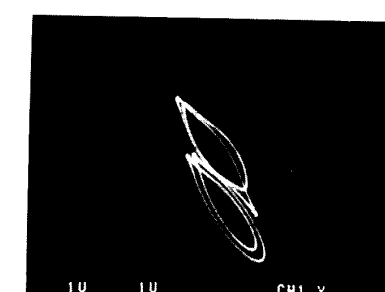
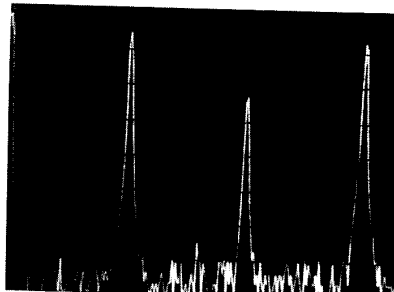
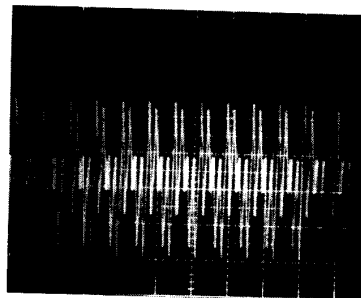


PARAMETERS:  $C_1 = .5$ ,  $C_2 = 100$ ,  $G_a = .599$ ,  $G_b = .77$

$R = .000929$ ,  $R_0 = -1.4286$ ,  $L = .136$

LYAPUNOV EXPONENTS:  $\lambda_1 = 0$ ,  $\lambda_2 = -.01$ ,  $\lambda_3 = -.04$

Fig.12 Experimental results (see the caption of Fig.2 for explanation) for the set of parameters as indicated.

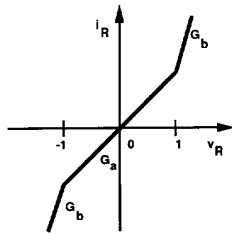
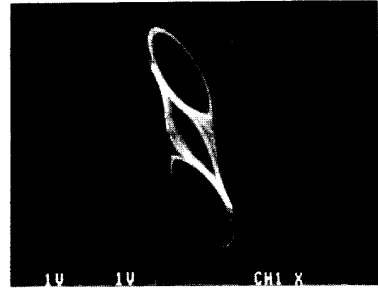
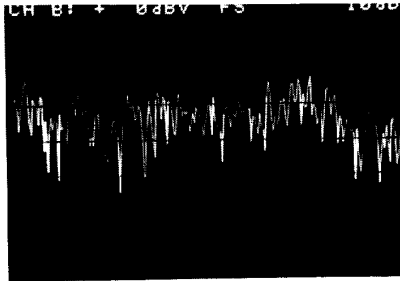
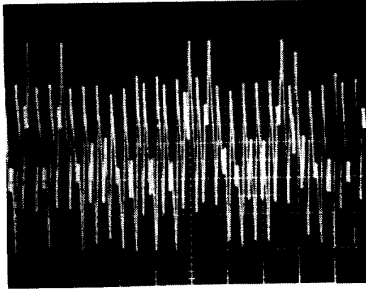


PARAMETERS:  $C_1 = .35$ ,  $C_2 = 100$ ,  $G_a = .599$ ,  $G_b = .77$

$R = .000929$ ,  $R_0 = -1.4286$ ,  $L = .136$

LYAPUNOV EXPONENTS:  $\lambda_1 = 0$ ,  $\lambda_2 = -.01$ ,  $\lambda_3 = -.04$

Fig.13 Experimental results (see the caption of Fig.2 for explanation) for the set of parameters as indicated.

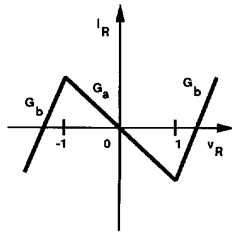
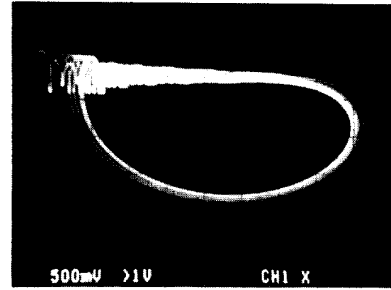
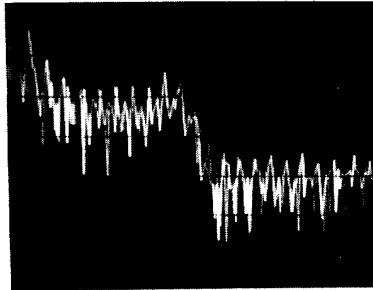
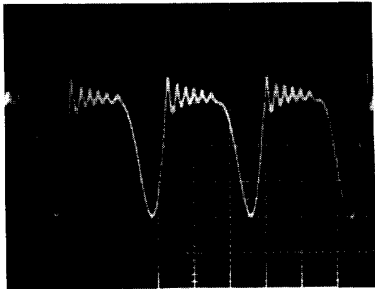


PARAMETERS:  $C_1 = .28$ ,  $C_2 = 100$ ,  $G_a = .599$ ,  $G_b = .77$

$R = .000929$ ,  $R_0 = -1.4286$ ,  $L = .136$

LYAPUNOV EXPONENTS:  $\lambda_1 = .01$ ,  $\lambda_2 = 0$ ,  $\lambda_3 = -.09$

**Fig.14** Experimental results (see the caption of Fig.2 for explanation) for the set of parameters as indicated.

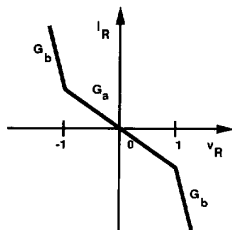
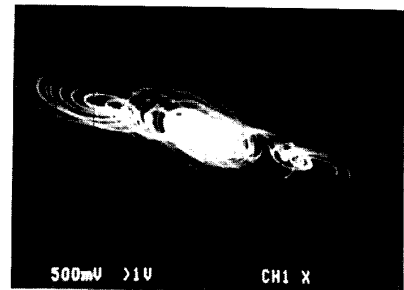
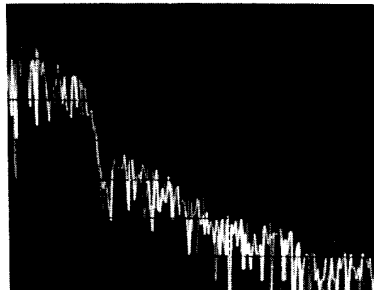
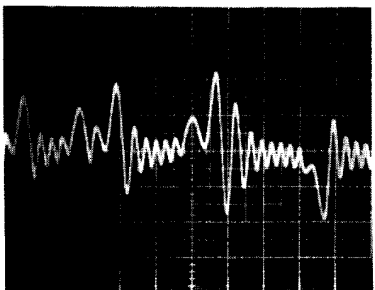


PARAMETERS:  $C_1 = 1$ ,  $C_2 = -1.0837$ ,  $G_a = -3.1935$ ,  $G_b = .0064$

$R = .02947$ ,  $R_0 = 0.0349$ ,  $L = -.0275$

LYAPUNOV EXPONENTS:  $\lambda_1 = .17$ ,  $\lambda_2 = 0$ ,  $\lambda_3 = -1.93$

**Fig.15** Experimental results (see the caption of Fig.2 for explanation) for the set of parameters as indicated.



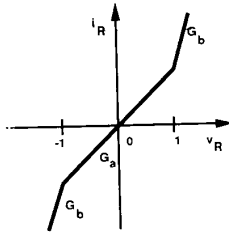
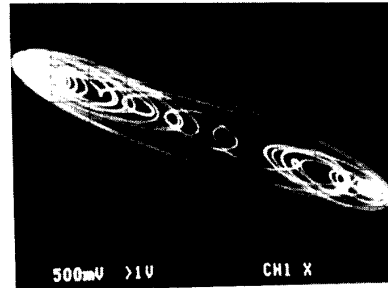
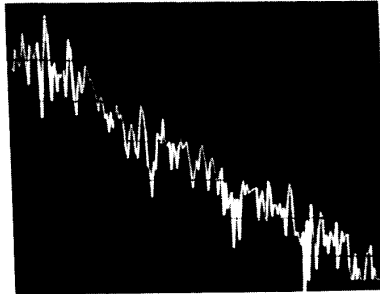
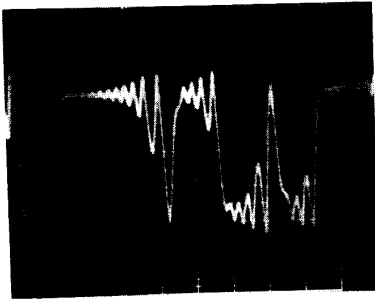
PARAMETERS:  $C_1 = 1$ ,  $C_2 = -1.3184$ ,  $G_a = -1.4925$ ,  $G_b = -.1871$

$R = .1502$ ,  $R_0 = 1.5866$ ,  $L = -2.3642$

LYAPUNOV EXPONENTS:  $\lambda_1 = .18$ ,  $\lambda_2 = 0$ ,  $\lambda_3 = -.60$

**Fig.16** Experimental results (see the caption of Fig.2 for explanation) for the set of parameters as indicated.



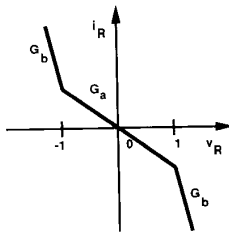
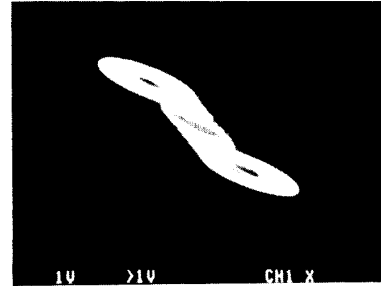
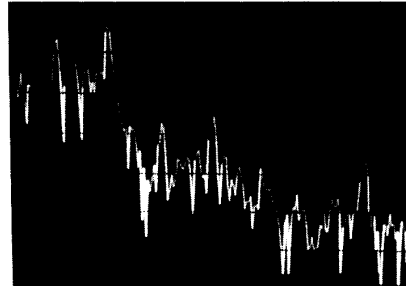
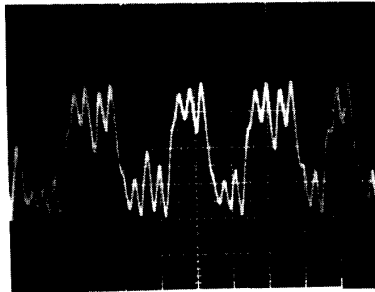


PARAMETERS:  $C_1=1$ ,  $C_2=-1.4245$ ,  $G_a=.2065$ ,  $G_b=.5247$

$R = -.3463$ ,  $R_0 = -3.7953$ ,  $L = -5.8026$

LYAPUNOV EXPONENTS:  $\lambda_1 = 0.10$ ,  $\lambda_2 = 0$ ,  $\lambda_3 = -.20$

Fig.17 Experimental results (see the caption of Fig.2 for explanation) for the set of parameters as indicated.

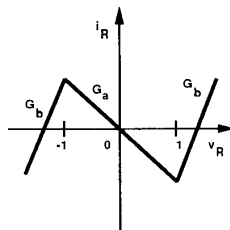
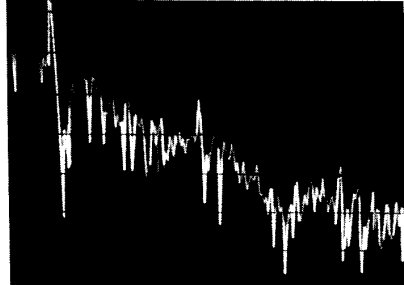
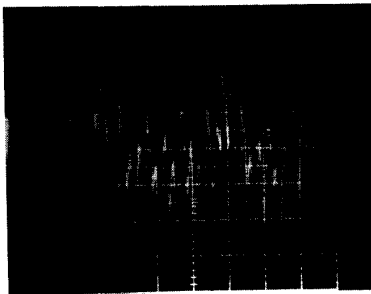


PARAMETERS:  $C_1=1$ ,  $C_2=9.3515$ ,  $G_a=-3.4429$ ,  $G_b=-2.1849$

$R = .33065$ ,  $R_0 = .00036$ ,  $L = .006913$

LYAPUNOV EXPONENTS:  $\lambda_1 = .07$ ,  $\lambda_2 = 0$ ,  $\lambda_3 = -.71$

Fig.18 Experimental results (see the caption of Fig.2 for explanation) for the set of parameters as indicated.

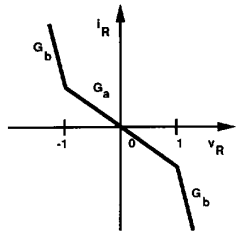
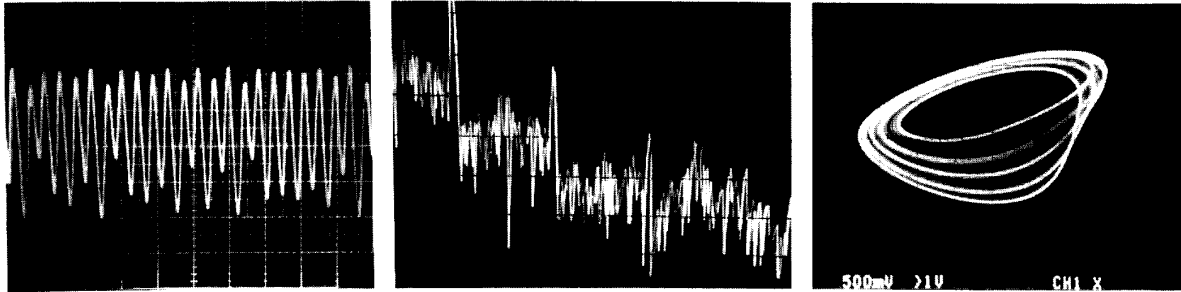


PARAMETERS:  $C_1=1$ ,  $C_2=3.7091$ ,  $G_a=-2.204$ ,  $G_b=.1439$

$R = 1.2544$ ,  $R_0 = -.0447$ ,  $L = .2423$

LYAPUNOV EXPONENTS:  $\lambda_1 = .06$ ,  $\lambda_2 = 0$ ,  $\lambda_3 = -.28$

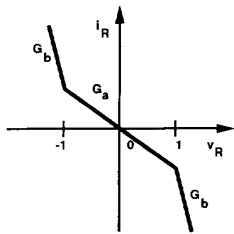
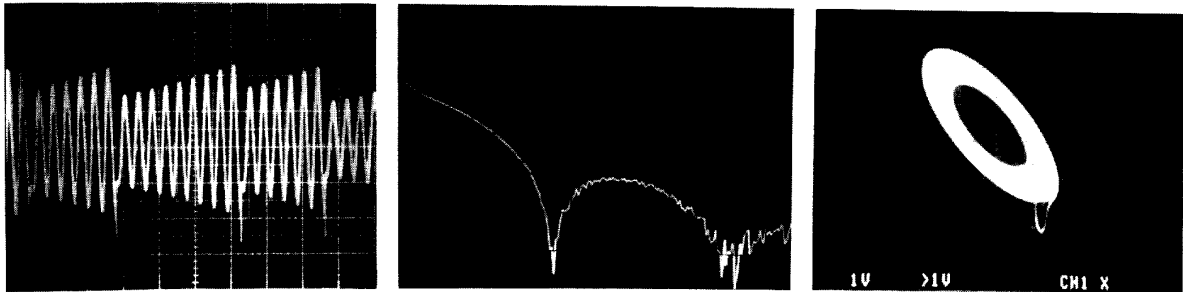
Fig.19 Experimental results (see the caption of Fig.2 for explanation) for the set of parameters as indicated.



PARAMETERS:  $C_1= 1, C_2= 6.5792, G_a= -2.8922, G_b= -1.5962$   
 $R = .4087, R_0= -.00167, L= .1008$

LYAPUNOV EXPONENTS:  $\lambda_1 = .06, \lambda_2 = 0, \lambda_3= -.74$

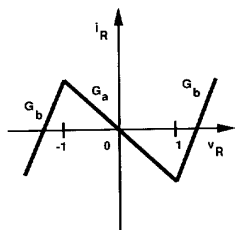
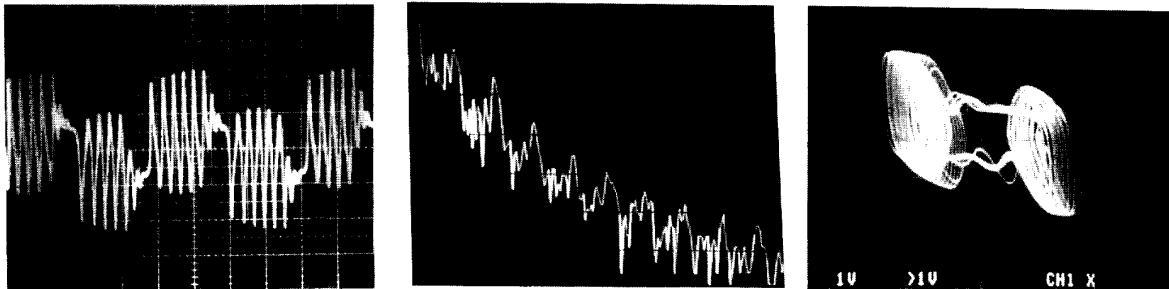
**Fig.20** Experimental results (see the caption of Fig.2 for explanation) for the set of parameters as indicated.



PARAMETERS:  $C_1= 1, C_2= -17.389, G_a= -32.257, G_b= -9.677$   
 $R = .0473, R_0= 0.0349, L= -.0275$

LYAPUNOV EXPONENTS:  $\lambda_1 = .05, \lambda_2 = 0, \lambda_3= -8.89$

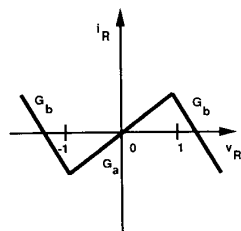
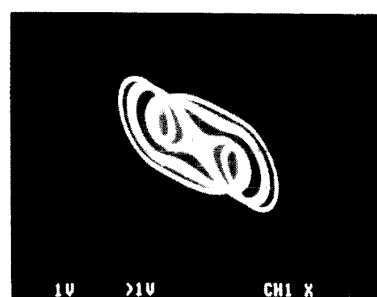
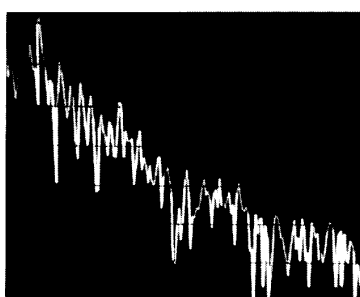
**Fig.21** Experimental results (see the caption of Fig.2 for explanation) for the set of parameters as indicated.



PARAMETERS:  $C_1= 1, C_2= -1.3018, G_a= -.2892, G_b= .8156$   
 $R = -.5846, R_0= -1.2758, L= 32.689$

LYAPUNOV EXPONENTS:  $\lambda_1 = .02, \lambda_2 = 0, \lambda_3= -0.05$

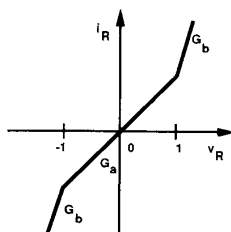
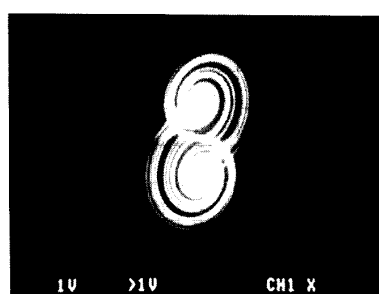
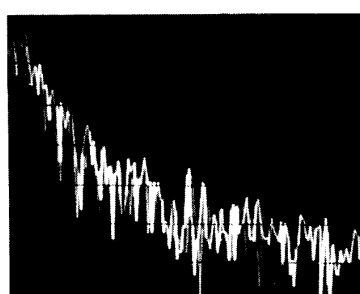
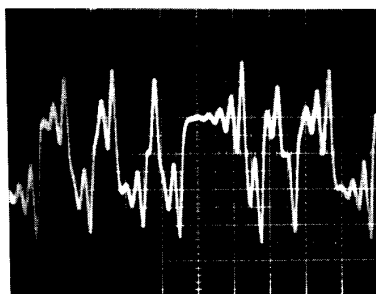
**Fig.22** Experimental results (see the caption of Fig.2 for explanation) for the set of parameters as indicated.



PARAMETERS:  $C_1=1$ ,  $C_2=-1.4589$ ,  $G_a=2.2668$ ,  $G_b=-.9541$   
 $R=.5375$ ,  $R_0=1.8562$ ,  $L=4.5284$

LYAPUNOV EXPONENTS:  $\lambda_1=.05$ ,  $\lambda_2=0$ ,  $\lambda_3=-.87$

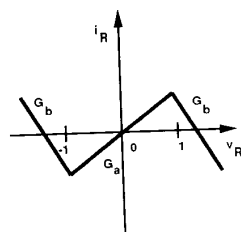
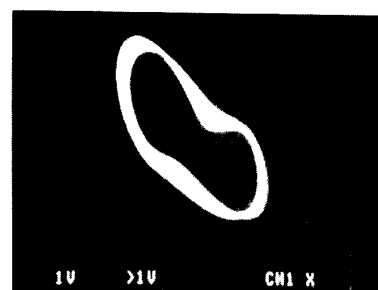
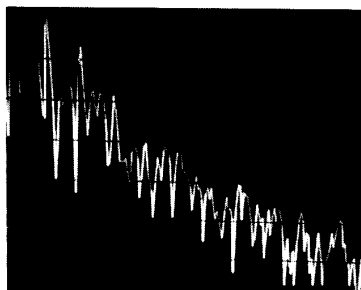
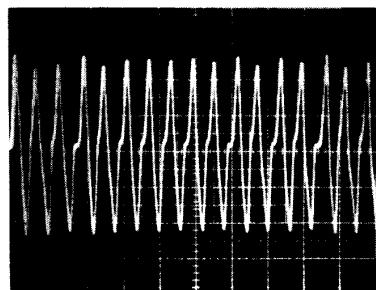
**Fig.23** Experimental results (see the caption of Fig.2 for explanation) for the set of parameters as indicated.



PARAMETERS:  $C_1=1$ ,  $C_2=-4.8989$ ,  $G_a=11.045$ ,  $G_b=4.1057$   
 $R=-.2265$ ,  $R_0=-.0000737$ ,  $L=.136$

LYAPUNOV EXPONENTS:  $\lambda_1=.15$ ,  $\lambda_2=0$ ,  $\lambda_3=-.98$

**Fig.24** Experimental results (see the caption of Fig.2 for explanation) for the set of parameters as indicated.



PARAMETERS:  $C_1=1$ ,  $C_2=-1.3635$ ,  $G_a=2.3282$ ,  $G_b=-.8982$   
 $R=1.9775$ ,  $R_0=.555$ ,  $L=4.8052$

LYAPUNOV EXPONENTS:  $\lambda_1=.05$ ,  $\lambda_2=0$ ,  $\lambda_3=-.75$

**Fig.25** Experimental results (see the caption of Fig.2 for explanation) for the set of parameters as indicated.